HHS Public Access

Author manuscript

Dev Cell. Author manuscript; available in PMC 2024 May 22.

Published in final edited form as:

Dev Cell. 2023 May 22; 58(10): 885–897.e4. doi:10.1016/j.devcel.2023.03.013.

Beclin-1-Dependent Autophagy but Not Apoptosis Is Critical for Stem Cell Mediated-Endometrial Programming and the Establishment of Pregnancy

Pooja Popli[1], **Suni Tang**[1], **Sangappa B. Chadchan**[1], **Chandni Talwar**[1], **Edmund B. Rucker III**[2], **Xiaoming Guan**[3], **Diana Monsivais**[1], **John P. Lydon**[4], **Christina L. Stallings**[5,6], **Kelle H Moley**[7,8], **Ramakrishna Kommagani**[1,9,10,*]

[1]Department of Pathology and Immunology, Baylor College of Medicine, One Baylor Plaza, Houston, TX 77030, USA.

[2]Department of Biology, University of Kentucky, Lexington, KY 40506, USA.

[3]Department of Obstetrics and Gynecology, Baylor College of Medicine, One Baylor Plaza, Houston, TX 77030, USA.

[4]Department of Molecular and Cellular Biology, Baylor College of Medicine, One Baylor Plaza, Houston, TX 77030, USA.

[5]Department of Molecular Microbiology, Washington University School of Medicine, St. Louis, MO, 63110, USA.

[6]Center for Women's Infectious Disease Research, Washington University School of Medicine, St. Louis, MO, 63110, USA.

[7]Department Obstetrics and Gynecology, Washington University School of Medicine, St. Louis, MO, 63110, USA.

[8]Center for Reproductive Health Sciences, Washington University School of Medicine, St. Louis, MO, 63110, USA.

[9]Department of Molecular Virology and Microbiology, Baylor College of Medicine, One Baylor Plaza, Houston, TX 77030, USA.

[10]Lead contact

[*]**Correspondence to:** Ramakrishna Kommagani, Associate Professor, Dept. of Pathology and Immunology, Dept. of Molecular Virology and Microbiology, Alkek Center for Metagenomics and Microbiome Research, T228A, One Baylor Plaza, Baylor College of Medicine, Houston, TX, 77030, Rama.Kommagani@bcm.edu, Phone: (713)-798-5085, Fax: 713-798-5838.

Author contributions

PP and RK designed experiments, conducted most of the studies, interpreted the data and wrote the manuscript. ST, SBC, and CT conducted some of the experiments. EBR, XG, DM, JP, CLS and KHM provided critical reagents for the study. RK conceived the project, supervised the work, and wrote the manuscript. All authors critically reviewed the manuscript.

Declaration of interests

The authors have declared that no conflict of interest exists.

Summary

The human endometrium shows a remarkable regenerative capacity that enables cyclical regeneration and remodeling throughout a woman's reproductive life. Although early postnatal uterine developmental cues direct this regeneration, the vital factors that govern early endometrial programming are largely unknown. We report that Beclin-1, an essential autophagy-associated protein plays an integral role in uterine morphogenesis during the early postnatal period. We show that conditional depletion of Beclin-1 in the uterus triggers apoptosis and causes progressive loss of $Lgr5^{+}$/$Aldh1a1^{+}$ endometrial progenitor stem cells, with concomitant loss of Wnt signaling, crucial for stem cell renewal and epithelial gland development. Beclin-1 knock-in (*Becn1* KI) mice with disabled apoptosis exhibit normal uterine development. Importantly, restoration of Beclin-1-driven autophagy but not apoptosis promotes normal uterine adenogenesis and morphogenesis. Together, the data suggest that Beclin-1-mediated autophagy acts as a molecular switch that governs the early uterine morphogenetic program by maintaining the endometrial progenitor stem cells.

Graphical Abstract

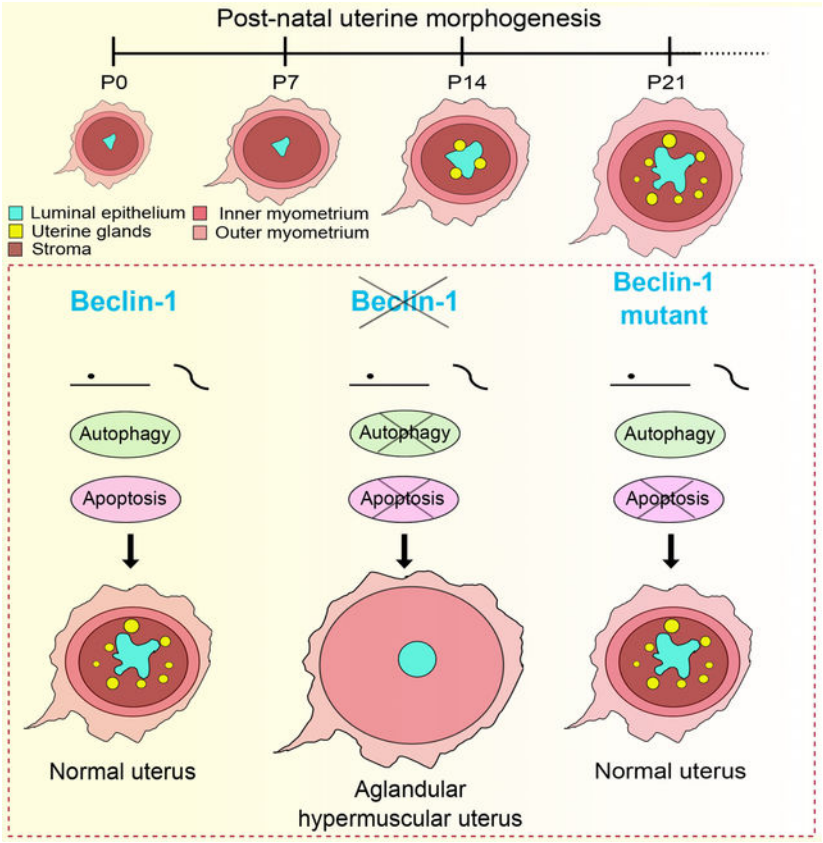

eTOC Blurb

Popli et al. discover that intrinsic autophagy is central to uterine morphogenesis, which is critical for establishing a successful pregnancy. Further, stem cell mediated-endometrial programming requires Beclin-1-dependent autophagy but not apoptosis. Defining the molecular mechanisms

underlying uterine morphogenesis will aid in developing strategies to diagnose and prevent early pregnancy loss.

Keywords

Autophagy; endometrium; beclin-1; stem cells; morphogenesis

Introduction

The uterus is composed of a multitude of different cell types organized into a hierarchy that undergoes dynamic changes to create a microenvironment conducive to embryo implantation. Each cell type among the heterogeneous populations plays a crucial role in establishing pregnancy; for example, endometrial epithelial cells undergo proliferation in response to high estrogen levels to facilitate implantation. Subsequently, endometrial stromal cells (ESCs) under high progesterone levels proliferate and differentiate into secretory decidualized cell types[1,2]. The decidualized ESCs then provide an appropriate environment for trophoblast invasion and secrete factors that are critical for the embryo's survival and placentation[3]. Another important cell type is the glandular epithelium, which produces essential factors and secretes necessary proteins to nourish developing embryos[4,5]. In the course of these sequential hormone-triggered cellular events, each uterine cell type (epithelium, stroma, and glands) displays robust cellular transformation and undergoes different cellular events, including proliferation, death[6,7], and differentiation, to ensure a successful pregnancy. Given the high rates of cell division and differentiation in the uterus during early pregnancy events, energy requirements, and metabolic rates tend to be high[8]. Thus, maintaining both energy and metabolic homeostasis in utero during these events relies on the ability of cells to sense and respond to changes in the availability of nutrients. Functioning as a major prosurvival mechanism, autophagy is one of the key cellular responses that gets upregulated rapidly in response to nutrient deprivation and high energy demands associated with the rapid proliferation and differentiation of cells[9,10].

There is also evidence that autophagy is highly active during the early development stages of pluripotency regulation and stem cell differentiation[11,12], but also fundamental to subsequent morphogenetic processes that together with apoptosis are decisive in tissue remodeling and shaping the embryo's organization[13–17]. Moreover, the autophagic process likely protects cells during metabolic stress and nutrient deprivation that occurs during tissue remodeling[13,18,19]. However, whether autophagy plays any role in stem cell-based endometrial programming and morphogenesis is not known.

Beclin-1 is the mammalian ortholog of yeast Atg6/Vps30 and was identified as a Bcl-2-interacting protein from a yeast two-hybrid screen[20]. Beclin-1 acts as an interface for three different cellular cascades- autophagy, differentiation, and apoptosis[21]. While the basal Beclin-1 level does not cause autophagy or differentiation, depletion of Beclin-1 derails both the autophagy and differentiation process leading to the activation of apoptosis[21,22]. Importantly, the interaction between Beclin-1 and the antiapoptotic protein, Bcl-2, and Bcl-xL governs the direction of Beclin-1-driven apoptotic and autophagic processes[23]. Further,

depending upon the nature of the stimuli, Beclin-1 engages in different cellular processes, e.g., under non-autophagic stimuli, the Beclin-1-Bcl-XL complex becomes apoptotic or anti-autophagic[24,25], and under autophagic stimuli, Beclin-1-Bcl-XL complex becomes antiapoptotic and autophagic[21].

In the present study, we investigated the role of Beclin-1 dependent autophagy in uterine development and, the impact on the establishment of pregnancy. We found that abrogation of autophagy in the uterus via deletion of *Becn1* resulted in infertility due to impaired uterine receptivity, and embryo implantation. In addition, molecular analysis of uteri from different postnatal (PN) ages indicated severe adenogenesis and uterine maturation defects in *Becn1* cKO mice. Mechanistically, we report that Beclin-1-dependent autophagy but not apoptosis is crucial for uterine maturation. These results demonstrate that intrinsic autophagy is an important regulator of uterus development and morphogenesis, which is critical for establishing a successful pregnancy.

Results

Conditional ablation of *Becn1* in reproductive tract results in infertility despite normal ovarian function

To identify the role of Beclin-1 in uterine functions, we generated *Becn1* reproductive tract-specific conditional knockout (*Becn1* cKO) mice, by crossing *Becn1*$^{flox/flox}$ mice with mice expressing Cre recombinase under the control of progesterone receptor promoter (Figure 1A). Previous studies indicated that PR-Cre expresses postnatally in the anterior lobe of pituitary glands, the corpus luteum, oviducts, and epithelial, stromal, and myometrial cellular compartments of uteri[26]. To determine the extent of knockout, we determined *Becn1* expression from different tissue samples including uterus, ovary, and liver of virgin mice. We found that *Becn1* expression at mRNA and protein levels was depleted in uteri from adult *Becn1* cKO mice compared to control mice, which was not the case for ovary and liver (Figure 1B & C). Further, immunohistochemistry analysis showed that levels of Beclin-1 protein were efficiently depleted from both the epithelial and stromal compartments of cKO uteri compared to the corresponding age-matched control uteri (Figure 1D). In addition, we did not find any difference between ER-α and PR expression in the uteri of 8-week-old adult control and cKO mice (Figure S1 A & B).

Next, to evaluate the impact of *Becn1* ablation on female fertility, we mated 8-week-old female mice (n = 5 for control and n = 6 for cKO) with virile wild-type male mice (Table 1). In six-month breeding trials, *Becn1* cKO females delivered no litters, whereas control females showed normal breeding activity during the test period and delivered an average of 8.6±2.52 pups per litter ($P \leq 0.05$) as shown in Figure 1E, indicating an indispensable role for *Becn1* in female fertility. Furthermore, wet uterine weights of *Becn1* cKO were much lower than control females (Figure 1F).

Since PR-Cre also expresses in the granulosa cells of pre-ovulatory follicles[26], and *Becn1* is shown to play an important role in the ovary[27], we examined ovarian function as well. Histological examination of ovaries from adult females showed no overt differences between *Becn1* cKO and control mice (Figure 1G). In addition, no significant differences in serum

estradiol (E2) and progesterone (P4) levels were noted in *Becn1* cKO compared to control mice (Figure 1H). Furthermore, superovulation of 4-week-old mice showed no significant difference in the number of oocytes released from both control and *Becn1* cKO mice (Figure 1I). *Becn1* cKO mice are infertile but showed normal ovarian function suggesting fertility defects likely caused by uterine defect. To determine this, we first assessed Beclin-1 expression in the uterus during early pregnancy events. Considerable expression of Beclin-1 observed in uteri from day 1 of pregnancy, which was not obvious in uteri from day 2 of pregnancy (Figure S2A). However, by day 3 and 4 of pregnancy, Beclin-1 levels reappeared with elevated expression in luminal epithelium, glandular epithelium, and stroma of pregnant uteri. Similarly, *Becn1* m-RNA levels varied in D1-D5 pregnant uteri (Figure S2B).

Loss of *Becn1* results in impaired embryo implantation and uterine receptivity in mice

To determine the effects of *Becn1* loss on uterine functions during pregnancy, we measured the implanting embryos from D-5 pregnant uteri. While several implantation sites were observed in control uteri at 5 dpc none were present in uteri of *Becn1* cKO mice (**black arrows**, Figure 2A). Histological analysis of the implantation sites in the control mice demonstrated that embryos attached properly to the luminal epithelium (LE), whereas *Becn1* cKO mice had unattached embryos floating within the uterine lumen (Figure 2B). Given the impaired embryo implantation in *Becn1*-cKO mice, we assessed the expression of the key uterine receptivity marker: mucin1 (MUC1) in the uterine luminal epithelium on day 5 of implantation (Figure 2C). For a uterus to be receptive to the embryo, expression of MUC1 must be locally removed from the luminal epithelium[28,29]. In cKO mice, the uteri appear non-receptive with the retention of MUC1 expression in the luminal epithelium (Figure 2C, S3). However, m-RNA levels of both *Esr1* and *Pgr* were comparable in both *Becn1* cKO and control uteri (Figure S3).

For successful embryo attachment and implantation into the uterus, the uterus must change from a non-receptive state to a receptive state under the controlled influence of steroid hormones. Thus, to assess the effects of *Becn1* knockout on the uterine response to E2 and P4, an established hormone-induced uterine receptivity experiment was employed[30] (Figure 2E). Control and *Becn1* cKO mice showed considerable epithelial proliferation in response to E2 treatment, as evident from similar Ki-67 staining in their uteri (Figure 2E). Consistently, E2 treatment induced expression of *Igf1*, a well-known marker for estrogen response in uterine epithelial proliferation[31] (Figure 2F). However, P4-mediated stromal cell proliferation was significantly blunted in the *Becn1* cKO uteri compared to control uteri (Figure 2E), indicating that *Becn1* might be essential for P4-mediated but not for E2-mediated actions during uterine receptivity.

Becn1 is required for postnatal uterine gland development

While carrying out these uterine-specific reproduction assays, we observed a lack of glands in adult *Becn1* cKO uteri (Figure 2A, 2C, and S1A). In a normal murine uterus, endometrial glands start budding from luminal epithelium by postnatal D7 (PND7), appear in the uterus by PND14, grow in number to branch out, and differentiate as they mature[32,33] (Figure 3A). Given the significance of uterine structures in overall uterine functions and fertility[34–39], we

wondered whether Beclin-1 is necessary for the appropriate gland development and uterine morphogenesis.

To dissect the role of Beclin-1 in postnatal uterine development, we first assessed the expression of Beclin-1 in the uteri collected during a critical window of gland development (1- to 3 weeks after birth) (Figure 3B). We found that Beclin-1 expresses spatio-temporally in all the essential uterine structures including luminal epithelium, glandular epithelium, and stroma. Since we used a PR-Cre mouse model for ablating Beclin-1, we analyzed PR expression during uteri development (Figure S4). Foxa2 is a transcription factor that uniquely expresses in the glandular epithelium of uterus and is a critical regulator of postnatal uterine gland differentiation in mice[34,35]. Analysis of uteri from different postnatal ages showed the absence of Foxa2 positive glands in *Becn1* cKO uteri compared to age-matched controls, indicating an indispensable role for Beclin-1 in uterine gland development (Figure 3C &D).

Loss of *Becn1* leads to undifferentiated stroma and myometrium resulting in hyper-muscular uteri

Postnatal morphogenesis of uteri is associated with coordinated development of the endometrial glands from the LE, organization, and differentiation of mesenchyme into endometrial stroma, and myometrium[40,41]. Therefore, the uteri of *Becn1* mice were histologically analyzed from endometrium and myometrium using epithelial (Cytokeratin KRT8-positive), stromal (Vimentin-positive), and myometrial (α-Smooth muscle active (SMA) positive,) markers at various PN developmental ages. From 2-weeks onwards, *Becn1* cKO mice showed both the endometrial and myometrial defects at the gross level and these developmental defects persisted over time (Figure S5A). Subsequent analysis of the 3-weeks PN age in control uteri showed well-organized myometrial layers and stromal compartments. However, distinct stromal and myometrial compartments could not be identified in *Becn1* cKO uteri as evident from the smooth muscle actin and vimentin staining (Figure 4A &B). Instead, actin-positive cells seemed to occupy a large uterine surface area with a concomitant decrease in vimentin-positive stromal area in cKO uteri (Figure 4A &B).

With the progression of age, control uteri displayed a mature uterine phenotype with all the differentiated compartments. In contrast, cKO uteri exhibited an enhanced pattern of uterine histoarchitectural deformities. Specifically, the stromal compartment in cKO uteri was reduced with concomitant expansion of myometrium. By 12 weeks of the PN age, the cKO uteri showed a hyper-muscular phenotype with the SMA-positive myometrium occupying most (90%) of the uterine surface area (Figure 4A &B). Whereas well-organized myometrial layers with circular orientation in a defined ring were evident in control uteri, a disorganized myometrium with disoriented smooth muscle layers was observed in *Becn1* cKO uteri (Figure S5B).

To identify the potential mechanism underlying these uterine maturation defects prominent in *Becn1* cKO mice, we analyzed the expression of various key genes essential for orchestrating these uterine-specific processes during neo-natal stages. At the postnatal age of 2-weeks, mRNA levels of *Wnt7a*, *Wnt 5a*, *Wnt 11*, *Wnt 16*, *Fzd6*, *Fzd10*, *Msx1*, and

Msx2 decreased, whereas expression of Wnt 4 increased in *Becn1* cKO uteri compared with age-matched controls (Figure 4C). The transcript levels of these key genes were found to be consistently dysregulated in uteri of 3-week-old *Becn1* cKO mice compared to their corresponding controls (Figure 4C). These findings suggest a potential link between *Becn1* and Wnt signaling in governing the uterine maturation and adenogenesis.

Endometrial progenitor stem cell maintenance requires *Becn1* during early uterine morphogenesis

Uterine morphogenesis consists of robust proliferation of luminal epithelium and stromal cells during the first postnatal week followed by a steady decline as each uterine compartment differentiates[41,42]. To investigate whether the observed uterine maturation defects in *Becn1* cKO mice are due to impaired cellular proliferation in the epithelial and stromal compartments, we analyzed the proliferation status of the uterus during the most crucial period of maturation (from 1 to 3 week of the PN stage) by Ki-67 immunostaining (Figure 5A). Interestingly, the uterine epithelium and stroma were highly proliferative in both *Becn1* cKO and control uteri by 1 week of PN age. However, by 2 weeks, there was a substantial decrease in proliferation of both the epithelium and stroma of *Becn1* cKO uteri compared to their corresponding control uteri (Figure 5A). Conversely, by 3 weeks of age, when the uterus becomes more mature, uteri from all control mice maintained a low proliferation status in the epithelium/stromal compartment, indicating the beginning of the differentiation phase (Figure 5A), whereas uteri from *Becn1* cKO showed an abundant number of Ki-67+ cells in the epithelium and stromal compartments (Figure 5A, **left panel**, Figure S6). Upon quantification, uteri from 3-week-old *Becn1* cKO mice showed ~4-fold and ~3-fold more Ki-67+ cells in their epithelium and stroma respectively than the age-matched controls (Figure 5A, **right panel**) ($P \leq 0.05$; n=4–6).

Since, epithelial cell proliferation and apoptosis are tightly controlled during the critical period of uterine maturation, we assessed apoptosis and DNA damage by measuring cleaved caspase-3 and yH2AX respectively[43]. Interestingly, *Becn1* cKO uteri had a significantly higher number of cleaved caspase-3-positive luminal epithelial (KRT8-positive) cells compared to control mice (Figure 5B). Similarly, we also observed a greater number of uterine epithelial cells expressing γ-H2AX, indicating that *Becn1* depletion in the uterus increased the number of apoptotic uterine epithelial cells (Figure 5B).

Recent findings identified the expression of putative endometrial progenitor stem cell (EPSCs) markers including Aldehyde Dehydrogenase 1A1 (*Aldh1a1*), and leucine rich repeat containing G protein-coupled receptor 5 (*Lgr5*) in uterine luminal and glandular epithelium[44]. Given the adenogenesis defects in uteri of *Becn1* cKO, we tested whether *Becn1* is essential for the maintenance of these EPSCs in the uterus. During early uterine development, expression of Aldh1a1 starts to appear in the uterus by 7 days and is confined to the glandular epithelium by 3 weeks of postnatal uterine development (Figure 5C). However, in the absence of *Becn1*, expression of Aldh1a1 in uterine epithelium diminished at 2 weeks and 3 weeks, though a marginal level of expression was observed at 1 week of the postnatal age (Figure 5C). Consistently, reduced transcript levels of *Lgr5* and *Aldh1a1* were also noted in postnatal uteri from *Becn1* cKO (Figure 5D). Further, flow cytometry-based

assay was carried out to identify the ALDH1A1 positive epithelial cell population in the uteri of 2-week-old *Becn1* control and cKO mice (Figure 5E). Uterine cells treated with diethylaminobenzaldehyde (DEAB) (a specific ALDH inhibitor) were used as a negative control and the CD326 antibody was used for epithelial cell gating. With this FACS analysis, we noted 5.37% $ALDH1A1^{+}CD326^{+}$ cells in the control uteri and uteri from cKO mice have significantly lower number (~50%) of these $ALDH1A1^{+}CD326^{+}$ cells. Consistent with its inhibitory activity, DEAB treated control cells had no $ALDH1A1^{+}CD326^{+}$ positive (0.08%) cell population. These results clearly suggest that *Becn1* is essential for maintaining endometrial progenitor stem cells during early uterine morphogenesis

Pharmacological inhibition of autophagy inhibits uterine gland development in mice and human organoids

To substantiate findings from *Becn1 cKO* mice, we evaluated neonatal uterine gland development following selective inhibition of autophagy by treating mice pups with Spautin (a specific inhibitor of Beclin-1-mediated autophagy) (Figure 6A). Spautin treatment led to a significant reduction in Foxa2-positive glands in 2-week-old uteri compared to vehicle treated uteri (Figure 6A). Next, the effect of autophagy inhibition on human uterine organoids formation was evaluated by employing a well-established uterine organoid culture system, that recapitulates the *in-vivo* uterine gland development[45,46]. For this, human endometrial organoids were generated from primary human endometrial epithelial cells and then treated with either Control (vehicle), or E2, or E2+Spautin, or Spautin (Figure 6B). Whilst organoids grew adequately in the Vehicle or E2 treated groups, Spautin alone or in presence of E2 impaired the organoids growth (Figure 6C). Consistent with organoids growth, a reduced expression in both *PGR* (E2-target) and *FOXA2* was seen with Spautin treatment (Figure 6D). Importantly, Spautin decreased the expression of well-known endometrial progenitor stem cell markers: *LGR5* and *ALDH1A1* in human organoids (Figure 6D). Consistent with *in-vivo* findings from *Becn1* cKO mice, Spautin inhibited the proliferation of organoids as evident from the fewer Ki-67+ cells in the E2+Spautin group compared to the E2-treated group (Figure 6E). We also observed reduced number of FOXA2 and γ-H2AX-positive cells in E2+Spautin group compared to E2 treated organoids (Figure 6E). These results demonstrate that intrinsic autophagy is critical for the early uterine morphogenesis.

Beclin-1-mediated autophagy, but not apoptosis is required for postnatal uterine gland development and morphogenesis

It is important to note that Beclin-1 maintains cellular homeostasis by playing a dual role in regulating both autophagy and apoptosis[23,47,48]. Caspase-mediated cleavage of Beclin-1 renders its apoptotic activity while disruption of the Beclin-1-Bcl-2 binding complex due to mutation in the BH3-only domain within Beclin-1 enhances its autophagic activity (Figure 7A). Given this dual role of Beclin-1, we investigated whether the Beclin-1-dependent autophagy or apoptosis is required for adenogenesis and uterine maturation during neonatal stages of mice. To determine the autophagy-specific role of Beclin-1 in adenogenesis and uterine maturation, we used genetically engineered *Becn1* KI mice with a targeted F121A mutation that decreases its interaction with the negative regulator, Bcl-2, leading to constitutively enhanced autophagy. Immunofluorescence analysis confirmed a significant

number of Foxa2 positive glandular structures budding from the luminal epithelium in both control and KI uteri (Figure 7B). Importantly, uteri from 2-week-old *Becn1* KI mice showed a distinct stromal and myometrial compartment with key marker genes similar to wild-type controls (Figure 7B & 7C). These findings suggest that postnatal uterine development may require active Beclin-1-dependent autophagy but not apoptosis (Figure 7D). To confirm this, we generated *Becn1* cKO/KI mice by crossing *Becn1*$^{flox/flox}$;PR$^{cre/+}$ male mice with *Becn1* KI female mice. Immunofluorescence analysis of uteri from 3-week-old mice showed a number of glands budding from the luminal epithelium (Figure 7E) as in their corresponding age-matched controls. Moreover, we observed well-differentiating stromal and myometrial compartments in *Becn1* cKO/KI uteri compared to cKO uteri, as evident from vimentin and smooth muscle α-actin staining shown in Figure 7E. Taken together, these results demonstrate that Beclin-1-mediated autophagy but not apoptosis governs postnatal uterine morphogenesis.

Discussion

In this study, we demonstrate that intrinsic autophagy is critical for stem cell-mediated endometrial programming and the establishment of pregnancy. Abrogation of intrinsic autophagy by conditional ablation of *Becn1* in the uterus resulted in infertility owing to altered uterine morphogenesis, eventually causing impaired embryo implantation, and uterine receptivity. Altered uterine maturation was accompanied by abnormal epithelial proliferation, excessive cell death likely of progenitor stem cells, leading to severe adenogenesis, and differentiation defects in *Becn1* cKO mice. Interestingly, induction of autophagy in *Becn1* cKO mice rescued their uterine phenotypic defects. Our study further expands on these findings and demonstrates that inhibition of Beclin-1-dependent autophagy by Spautin-1 inhibitor significantly reduced epithelial cell differentiation in human endometrial organoids as well. Together, these findings establish a critical role of intrinsic autophagy in maintaining endometrial homeostasis.

Uterine glands and their secretions are critical regulators of peri-implantation blastocysts survival and implantation, as well as the establishment of uterine receptivity in numerous species[49,50]. Several studies reported that the absence of glands caused infertility in adults[35,51]. The aglandular phenotype of *Becn1* cKO in our study further supports this notion that uterine glands are indispensable for establishing a successful pregnancy. Autophagy as an evolutionarily conserved mechanism is known to regulate morphogenesis of a number of organs, including the heart, lung, intestine, and brain[15,17,52–54]. During morphogenesis, enhanced autophagic degradation is often required to cope with the drastic cellular and tissue remodeling. Here, we report that autophagy likewise is crucial for neonatal uterine maturation, including glandular morphogenesis. Extensive uterine luminal epithelium proliferation is considered as a critical event for the development and differentiation of glands during early uterus maturation[37,43]. In our study, abrogation of *Becn1*-mediated autophagy caused abruptly proliferating uteri by 3-week of postnatal age, suggesting that *Becn1* cKO uteri continued proliferating and failed to undergo differentiation with increasing postnatal ages. A robust increase in apoptosis in the epithelial compartment further suggests that activation of aberrant proliferation might reflect a compensatory mechanism to fulfil the loss of apoptotic cells. Increased apoptosis has also been reported

for other conditional knock-out models of autophagy[9,55,56]. Failure to activate autophagy in response to stimuli is known to trigger apoptotic cell death[57]. Lack of autophagy in the uteri of *Becn1* cKO mice in response to high energy demands and metabolic requirements for proliferation may also contribute to apoptosis of the epithelial cells, eventually resulting in morphogenesis defects. Consistent with these findings in mice, reduced proliferation, and increased DNA damage of epithelial cells with Spautin treatment suggests that human organoids fail to undergo differentiation in the absence of autophagy. Additionally, mouse models with conditional deletion of Wnt signaling markers such as Wnt5a, Wnt7a, and beta-catenin 1 (Ctnnb1)[58–60] in the uterus displayed a similar uterine phenotype as observed in our study. Abrogation of several Wnt signaling markers in response to autophagy inhibition suggests a potential regulator axis between autophagy and Wnt signaling. However, more future studies are required to unravel the mechanism of autophagy-mediated regulation of Wnt signaling during uterine maturation.

The mammalian uterus differentiates from the fetal mullerian ducts and typically consists of a central tubular epithelium surrounded by an undifferentiated mesenchyme at birth. Postnatal morphogenesis of uteri includes coordinated development of the endometrial glands from the LE, organization, and differentiation of mesenchyme into the endometrial stroma, and myometrium[40,41]. Epithelial-mesenchymal interactions play a crucial role in the correct patterning of uteri during this period. Tissue recombinant experiments showed that the epithelium is developmentally dynamic and adopts either a uterine (simple columnar) or vaginal (squamous/stratified) epithelial fate depending upon the mesenchyme origin (uterine or vaginal)[61]. The mesenchyme further depends upon the epithelium for its differentiation as grafts of uterine mesenchyme failed to induce myometrial differentiation in the absence of the epithelium, while epithelia from different organs including the uterus were able to induce extensive myometrial differentiation in the uterine mesenchyme[62,63]. These findings suggest that while mesenchymal factors decide the fate of epithelium, the epithelium, in turn, regulates the mesenchymal differentiation. In our study, with progressive declines in *Becn1* levels with age, the mesenchyme fails to drive epithelial differentiation in the absence of autophagy, leading to aglandular phenotype and improper myogenesis in cKO uteri. The anomalous hyper-muscular phenotype in these mice further shows that Beclin-1 might be interacting with other proteins and assisting in maintaining a rigorous regulatory control on myometrium growth. Given the critical epithelial-mesenchymal interactions during the early uterine maturation phase, more future studies are required to comprehend compartment-specific roles of Beclin-1 and the paracrine signaling involved therein using uterine epithelial or mesenchyme-specific conditional knockout mice models.

In addition to postnatal morphogenesis, functional differentiation is another stage of differentiation that occurs in the uterus during estrus cycles or pregnancy and is regulated by steroid hormones, E2 and P4. In our study, diminished Beclin-1-mediated autophagy at the neonatal stage also impacted the functional differentiation of adult cKO uteri, and that could be the reason why these mice fail to establish pregnancy and undergo substantial cellular transformations (e.g., P4-mediated stromal cell proliferation) needed for a healthy pregnancy. Since early pregnancy events are strictly orchestrated by steroid hormones, altered expression of Beclin-1 during pregnancy indicates that hormones are likely involved in regulating its levels and may coordinate these events to help meet its high energy

demands. Another crucial event that has been recognized as a determinant of successful implantation in mice is apoptosis[6] where both uterine epithelial and stromal cells undergo cell death to facilitate embryo anchorage and access to the maternal blood supply. Given the dual function of Beclin-1, we posit that Beclin-1-dependent apoptosis might play an important role in mediating this event.

Another interesting feature of autophagy is its role in maintaining the pluripotency of adult stem cells. Under physiological conditions, stem cells largely remain quiescent and retain their stemness; nevertheless, they can either proliferate or differentiate to meet regenerative demands and maintain tissue homeostasis. Essential role of endometrial stem cells, e.g., *Lgr5*, *Aldh1a1*, for uterine gland development in mice have recently been identified[64–66]. However, the key process that drive stem cell-mediated morphogenetic processes in uterus are understudied. In our study, reduced expression of both *Lgr5* and *Aldh1a1* during the early uterine maturation phase suggests that Beclin-1 mediated autophagy might be important for the maintenance of these stem cells in uterus, and abrogation of this pathway might lead to gradual loss of stem cells. Moreover, *Lgr5* is also reported as a Wnt-dependent stem cell essential for uterine gland development in mice[64]. In our study, decreased Wnt signaling markers due to inhibition of *Becn1*-mediated autophagy might be responsible for loss of Lgr5-positive stem cells culminating in uterine development defects. These findings were further corroborated by reduced expression of LGR5 and ALDH1A1 in human endometrial organoids when treated with Spautin autophagy inhibitor. We show that Beclin-1-mediated autophagy might be crucial for maintaining endometrial stem cell maintenance and differentiation in the uterus.

Beclin-1 acts as an interface for three different cellular cascades: autophagy, differentiation, and apoptosis[21]. While the basal Beclin-1 level does not cause autophagy or differentiation, depletion of Beclin-1 cripples both autophagy and differentiation and activates apoptosis[21,22]. Depending on the nature of stimuli, Beclin-1 engages in different cellular processes. For instance, under non-autophagic stimuli, the Beclin-1-Bcl-XL complex is apoptotic or anti-autophagic[24,25], whereas under autophagic stimuli, Beclin-1-Bcl-XL is antiapoptotic but autophagic[21]. Contrary to these findings, there are reports suggesting that unlike other BH3-only proteins, Beclin-1 fails to antagonize anti-apoptotic functions of Bcl-2 even when it is overexpressed[67,68]. A previous study in this regard gained attention where the Beclin-1-Bcl-2 binding interaction was disrupted, resulting in activation of Beclin-1 mediated constitutive autophagy in mice and these mice showed improved cognition with Alzheimer's disease[69]. Enhanced autophagy in *Becn1* KI mice was also shown to promote neurogenesis and counteract the aging-related neural stem cell exhaustion[70]. In our study, rescue of the impaired uterine morphogenesis phenotype of *Becn1* cKO mice via constitutive activation of Beclin-1-mediated autophagy implies that Beclin-1-dependent autophagy (but not apoptosis) is important for proper uterine maturation, possibly via stem cell maintenance. In addition, there is the possibility that under the influence of continuous autophagy stimuli during the morphogenesis period, cellular energy sensors like mTOR might be phosphorylating the Bcl-XL and disrupting its interaction with Beclin-1, thereby inducing constitutive autophagy to meet the energy demands. Tracking the Beclin-1-dependent autophagy flux using bigenic *Becn1*$^{flox/flox}$ or *Becn1* KI mice along with either GFP-LC3 or mCherry-LC3 transgenic models (Moulis

and Vindis, 2017; Rocchi et al., 2017) will be highly intriguing and provide more hints for its role in mediating uterine-specific processes. Further, understanding the complex rheostat between Beclin-1-Bcl-2 autophagy/apoptosis regulatory axis warrants future investigations with lineage tracking mouse models coupled with advance biochemical studies.

Collectively, our study demonstrates that the Beclin-1-mediated autophagy pathway in the uterus is critical for proper differentiation of uterine compartments. Deficiency of intrinsic autophagy results in structurally abnormal uteri with maturation defects that lead to pregnancy failure. From a clinical point of view, understanding how autophagy is induced during uterine differentiation may help us to advance our knowledge of fertility-associated gynecological pathologies.

Limitations of the study

In this study, we demonstrated a role for Beclin-1 in post-natal uterine morphogenesis by ablating its expression in all compartments of the uterus. However, it is possible that Beclin-1 acts in a paracrine manner to govern the development of specific uterine cells, which could be elucidated by employing compartmental-specific Beclin-1-deficient mouse models of the uterus. Additionally, autophagic flux might undergo dynamic changes during the uterine morphogenesis process, a spatiotemporal regulation of which might not be totally dependent on Beclin-1. Thus, monitoring the Beclin-1-dependent autophagy flux using autophagy-monitoring and autophagy-deficient mice will provide the relative contribution of Beclin-1 in overall autophagy flux dynamics in the uterus.

STAR*METHODS

RESOURCE AVAILABILITY

Lead contact—Further information and requests for resources and reagents should be directed to and will be fulfilled by the lead contact, Ramakrishna Kommagani (rama.kommagani@bcm.edu).

Materials availability—The mouse lines generated (Beclin-1$^{f/f}$, Beclin-1 cKO and Beclin-1 cKO/KI) are available from the lead contact upon request.

Data and code availability

- All data to support the findings of this study are included in the paper and the supplemental information.
- The datasets used and/or analyzed during the current study are available from the corresponding author on reasonable request.
- Any additional information required to reanalyze the data reported in this paper is available from the lead contact upon reasonable request.

EXPERIMENTAL MODEL AND SUBJECT DETAILS

Animal care and use—All animal studies were approved by the Institutional Animal Care and Use Committee of Washington University School of Medicine, Saint Louis, MO,

USA and Use Committee of Baylor College of Medicine, Houston, TX, USA. Beclin-1 mice were a generous gift from Dr. Edmund B. Rucker 3rd at the Department of Biology, University of Kentucky, and previously described[27]. Beclin$^{flox/flox}$ mice, in which exons 1 and 2 are flanked by loxp sites, were bred to progesterone receptor cre (PR$^{cre/+}$) mice to generate (Beclin$^{flox/flox}$; PR$^{cre/+}$ mice), hereafter referred to as *Becn1* cKO mice. Both control and conditional knockout females were generated by crossing females carrying homozygous *Becn1*$^{flox/flox}$ alleles with *Becn1* cKO males. *Becn1*$^{F121A/F121A}$ (*Becn1* KI) mice were a generous gift from Dr. Christina Stallings at Washington University St. Louis and previously described[69]. The *Becn1*$^{F121A/F121A}$ female mice are fertile with no overt developmental defects as shown by earlier report[69]. *Becn1* cKO/KI mice were generated by crossing females carrying homozygous *Becn1*$^{F121A/F121A}$ alleles with *Becn1* cKO males. All transgenic mice were maintained on a C57BL/6 genetic background (The Jackson Laboratory, Bar Harbor, ME) to minimize variation in the gestation length. All experimental animals were housed 5 per cage in institutional animal facility in standard ventilated cages with free access to water and food and under a 12-hr light and dark cycle. Animals were handled according to an approved institutional animal care and use committee (IACUC) protocol number [AN-8890]. Cages were changed routinely, and the health of the mice was monitored daily, and only healthy mice were used for this study. Breeding was carried out in duos or trios. Mice were genotyped by PCR analysis of genomic DNA isolated from tail clippings using the gene-specific primers listed in STAR Methods.

Human Organoid Culture—All experiments involving human subjects were approved by the Institutional Review Board of Baylor College of Medicine (IRB ID #: H-21138). Tissue samples were collected from patients upon informed consent. Human organoids were established and maintained as described before[45]. Following passaging, 10,000 cells per Matrigel droplet were plated in 12-well plates (3 droplets per well) and allowed to establish into organoids over 4 days in organoid medium. To examine the effect of Beclin-1 dependent autophagy on E2-mediated organoids growth and differentiation, organoids were treated with either vehicle control (100% ethanol) or E2 (10 nM) or E2 (10 nM) + Spautin (15 μM) or Spautin (15 μM) alone for subsequent 2 days (Figure 6B). At the end of experiment, organoids were collected from each well and processed for transcript and immunofluorescence analysis.

Method Details

Fertility analysis and timed mating—Female fertility was assessed by mating cohorts of *Becn1* cKO experimental (n = 6) and control *Becn1* f/f (n = 5) females individually starting at 8 weeks of age with sexually mature males of proven fertility. The numbers of litters and pups were tracked over a 6-months period for each female. Pups per litter for each genotype are reported as mean ± SEM. For timed mating, the morning on which the copulatory plug was first observed was considered 1 dpc. To visualize implantation sites, mice received a tail vein injection of 50 μL of 1% Chicago Sky Blue dye (Sigma-Aldrich, St. Louis, MO, USA) at 5 dpc just prior to sacrifice.

Super-ovulation Analysis—Female mice at age of 4 weeks were injected with 5 IU pregnant mare serum gonadotropin (PMSG), followed by 5 IU human chorionic

gonadotropin (hCG) 44–46 h later. After an additional 18–22 h, the mice were sacrificed, and oviducts were isolated. Cumulus-oocyte complexes (COC) were removed from the oviducts and collected in M2 medium (Sigma-Aldrich). The number of COCs per female was counted and compared across genotypes.

Hormone Analysis—Blood was collected from virgin 8-week-old females before mice were sacrificed. Serum was separated from the blood by centrifugation and stored at −80°C before hormone analysis. Serum P4 and E2 levels were measured by using ELISA kits (Enzo life Sciences) according to the manufacturer's instructions.

Steroid hormone treatments—The hormonal profile of pregnancy at the time of implantation was simulated using a well-established experimental scheme[29,30,71]. Briefly, *Becn1* cKO and control mice at 8 weeks of age were bilaterally ovariectomized under ketamine anaesthesia with buprenorphine-SR as analgesics. Mice were rested for two weeks to allow all endogenous ovarian hormones to dissipate. Mice were then injected with 100 ng of estrogen (E2; Sigma-Aldrich) dissolved in 100 μl of sesame oil on two consecutive days and then allowed to rest for two days. At this point, mice were randomly divided into three groups of five: Vehicle-treated (E2 priming) mice received four consecutive days of sesame oil injections. E2 nidatory mice received three days of sesame oil injections followed by a single injection of 50 ng of E2 on the fourth day. The E2/P4 mice received 1 mg of progesterone (P4; Sigma-Aldrich) for three consecutive days followed by a single injection of 1 mg P4 plus 50 ng E2 on the fourth day. All hormones were delivered by subcutaneous injection in a 90:10 ratio of sesame oil: ethanol. Mice were euthanized 16 hours after the final hormone injection to collect the uteri. A small piece of tissue from one uterine horn was processed in 4% neutral buffered paraformaldehyde for histology, and the remaining tissue was snap-frozen and stored at −80 °C.

Hematoxylin and Eosin staining—Tissues were fixed in 4% paraformaldehyde, embedded in paraffin, and then sectioned (5 μm) with a microtome (Leica Biosystem, Germany). Tissue sections were deparaffinized, rehydrated, and stained with Hematoxylin and Eosin[72]. All the histology was performed on three sections from each tissue of individual mice, and one representative section image is shown in the respective figures.

Histological analysis—The collected uterine tissues were fixed in 4% paraformaldehyde and embedded in paraffin. Sections (5 μm) were immunostained (n = 5 per group)[72]. Briefly, after deparaffinization, sections were rehydrated in an ethanol gradient, then boiled for 20 min in citrate-buffer (Vector Laboratories Inc., CA, USA) for antigen retrieval. Endogenous peroxidase activity was quenched with Bloxall (Vector Laboratories Inc., CA, USA), and tissues were blocked with 2.5% goat serum in PBS for 1 hr (Vector Laboratories Inc., CA, USA). After washing in PBS three times, tissue sections were incubated overnight at 4°C in 2.5% goat serum containing the primary antibodies listed in STAR Methods. Sections were incubated for 1 hr with biotinylated secondary antibody, washed, and incubated for 45 min with ABC reagent (Vector Laboratories Inc., CA, USA). Color was developed with 3, 3'-diaminobenzidine (DAB) peroxidase substrate (Vector Laboratories Inc.), and sections

were counter-stained with hematoxylin. Finally, sections were dehydrated and mounted in Permount histological mounting medium (Fisher Scientific).

Immunofluorescence analysis—Formalin-fixed and paraffin-embedded sections were deparaffinized in xylene, rehydrated in an ethanol gradient, and boiled in citrate-buffer (Vector Laboratories Inc., CA, USA) for antigen retrieval. After blocking with 2.5% goat-serum in PBS (Vector laboratories) for 1 h at room temperature, sections were incubated overnight at 4°C with primary antibodies (STAR Methods) diluted in 2.5% normal goat serum. After washing with PBS, sections were incubated with Alexa Fluor 488-conjugated secondary antibodies (Life Technologies) for 1 h at room temperature, washed, and mounted with ProLong Gold Antifade Mountant with DAPI (Thermo Scientific). For quantification of Ki67, phospho-γH2AX, and cleaved caspase-3 positively stained cells, cells were counted manually in images taken at 40X magnification by two independent investigators blinded to treatment groups. Cells were counted in at least four different areas in uterine cross-sections and plotted as percent positive cells relative to total number of cells[71,72].

For quantification of Foxa2 positive glandular structures, number of glands was counted from four different areas of uterine cross-sections images taken at 100X magnification and the average number of glands from n=3 mice was presented[35].

Similarly, human organoids treated with Vehicle, E2, E2+Spautin, and Spautin alone were processed for immunofluorescence to detect the expression of various markers including Foxa2, Ki-67, and y-pH2AX. For quantification of Foxa2, Ki-67, and γH2AX positive cells, cells were counted manually in images taken at 400X magnification by two independent investigators blinded to treatment groups. Percent positive cells were plotted relative to total number of cells. Three independent experiments were performed and for each experiment, 7–10 organoids/group were counted[73]. All Immunofluorescence images were obtained using a Zeiss LSM 880 confocal microscope (10x and 40 x objective lens).

Western blotting—Protein lysates (40 μg per lane) were loaded on a 4–15% SDS-PAGE gel (Bio-Rad), separated in 1X Tris-Glycine Buffer (Bio-Rad), and transferred to PVDF membranes via a wet electro-blotting system (Bio-Rad), all according to the manufacturer's directions[74]. PVDF membranes were blocked for 1 hour in 5% non-fat milk in Tris-buffered saline containing 0.1% Tween-20 (TBS-T, Bio-Rad), then incubated overnight at 4°C with antibodies listed in STAR Methods in 5% BSA in TBS-T. Blots were then probed with anti-Rabbit IgG conjugated with horseradish peroxidase (1:5000, Cell Signaling Technology) in 5% BSA in TBS-T for 1 hour at room temperature. Signal was detected with the Pierce™ ECL Western Blotting Substrate (Millipore, MA, USA), and blot images were collected with a Bio-Rad ChemiDoc imaging system.

RNA Isolation and Quantitative Real-Time RT-PCR Analysis—Tissues/cells or organoids were lysed in RNA lysis buffer, and total RNA was extracted with the Purelink RNA mini kit (Invitrogen, Carlsbad, CA, USA) according to the manufacturer's instructions. RNA was quantified with a Nano-Drop 2000 (Thermo Scientific, Waltham, MA, USA). Then, 1 μg of RNA was reverse transcribed with the High-Capacity cDNA Reverse Transcription Kit (Thermo Scientific, Waltham, MA, USA). The amplified cDNA was

diluted to 10 ng/μl, and qRT-PCR was performed with primers listed in STAR Methods and TaqMan 2X master mix (Applied Biosystems/Life Technologies, Grand Island, NY) on a 7500 Fast Real-time PCR system (Applied Biosystems/Life Technologies). The delta-delta cycle threshold method was used to normalize expression to the reference gene 18S.

Treatment of mice with Spautin inhibitor—Spautin-1, a pharmacological agent that inhibits Beclin-1-mediated autophagy by interfering with its degradation, was used to study its effects during uterus development[75]. Specifically, Spautin-1 promotes Beclin-1 degradation, by acting as an antagonist for two ubiquitin-specific peptidases, USP10/USP13, which are known to regulate Beclin-1 deubiquitination in Vps34 complexes. Five-day_old C57BL/6 mice pups were injected daily intraperitoneally with Spautin inhibitor dissolved in 40% PEG-300 (40mg/kg body weight) till two weeks of postnatal age (Figure 6E). Dimethyl Sulfoxide with 40% PEG-300 was administered as vehicle.

Flow Cytometry—Uterus tissues single cell suspension was prepared using enzymatic digestion method[76]. Briefly, fresh uteri were dissected from female *Becn1* f/f (n=3) and cKO (n=4) two-weeks old pups. Uteri for each group were pooled, finely minced, and enzymatically digested with 0.5% w/v collagenase Type I (Sigma) in DMEM/F-12 medium (Gibco) and 0.05% deoxyribonuclease type I at 37°C for 1 h on a rotator. After one-hour, enzymes and cell debris were removed by centrifugation at 230g for 5 min, washed with ice-cold PBS followed by filtering of the single cell suspension through a 100 μm cell strainer (BD Bioscience). The resultant single cell suspension (1×10^6) was resuspended in 1% v/v fetal bovine serum (FBS) (Life Technologies) in PBS (FBS/PBS) and stained with the ALDEFLUOR™ reagent from the ALDEFLUOR™ assay kit (Stem Cell Technologies, Vancouver, BC, Canada) according to the manufacturer's protocol and labelled with brilliant-violet conjugated CD326 antibody. As negative control, for each sample of cells an aliquot was treated with diethylaminobenzaldehyde (DEAB), a specific ALDH inhibitor provided with the kit. The flow cytometry gating was established using the negative controls: unstained cells, the ALDEFLUOR-stained cells treated with DEAB and Fluorochrome-conjugated isotype controls. Flow cytometry analysis was performed using a FACSCanto II flow cytometer with FACSDiva Software (BD Biosciences, Le Pont-de-Claix, France).

Quantification and Statistical Analysis—A two-tailed paired student t-test was used to analyze data from experiments with two experimental groups and one-way ANOVA followed by Tukey's post hoc multiple range test was used for multiple comparisons. All data are presented as mean ± SE. GraphPad Prism 9 software was used for all statistical analyses. All the statistical details related to tests performed and sample size, p-values can be found in the corresponding figure legends. To ensure the reproducibility of our findings, experiments were replicated in a minimum of three independent samples, to demonstrate biological significance, and at least three independent times to ensure technical and experimental rigor and reproducibility.

Supplementary Material

Refer to Web version on PubMed Central for supplementary material.

Acknowledgments

We thank Dr. Robert Michael Lawrence (Senior Editor at Baylor College of Medicine) for assistance with manuscript editing. Cartoons in Figures 6, and 7 were downloaded from BioRender.com. This work was funded, in part, by National Institutes of Health/National Institute of Child Health and Human Development (grants R01HD102680, R01HD104813 and R01HD065435) to RK and R01 HD105800 to Diana Monsivais (D.M.). D.M. Ph.D. holds a Next Gen Pregnancy Award (NGP10125) from the Burroughs Wellcome Fund. This work was also funded by NIH Awards NIAID R01 AI132697 and U19 AI142784 to Dr. Christina L. Stallings. We thank Venkata Naga Goutham Davuluri (Department of Pathology & Immunology, Baylor College of Medicine, Houston, TX) for assisting with flow cytometry. This project was supported by the Cytometry and Cell Sorting Core at Baylor College of Medicine with funding from the CPRIT Core Facility Support Award (CPRIT-RP180672), the NIH (CA125123 and RR024574) and the assistance of Joel M. Sederstrom.

Non-standard Abbreviations

WT	Wild Type
***Becn1* cKO**	Beclin-1 conditional knockout
***Becn1* KI**	Beclin-1 Knock-in
ESCs	Endometrial stromal cells
PR	Progesterone receptor
ERα	Estrogen receptor alpha
dpc	Days post coitum
E2	Estrogen
P4	Progesterone
PNDs	Postnatal days
EPSCs	endometrial progenitor stem cells
SPA	Spautin

References

1. Matsumoto H (2017). Molecular and cellular events during blastocyst implantation in the receptive uterus: clues from mouse models. J Reprod Dev 63, 445–454. 10.1262/jrd.2017-047. [PubMed: 28638003]
2. Robertshaw I, Bian F, and Das SK (2016). Mechanisms of uterine estrogen signaling during early pregnancy in mice: an update. J Mol Endocrinol 56, R127–138. 10.1530/JME-15-0300. [PubMed: 26887389]
3. Ramathal CY, Bagchi IC, Taylor RN, and Bagchi MK (2010). Endometrial decidualization: of mice and men. Semin Reprod Med 28, 17–26. 10.1055/s-0029-1242989. [PubMed: 20104425]
4. Filant J, and Spencer TE (2014). Uterine glands: biological roles in conceptus implantation, uterine receptivity and decidualization. Int J Dev Biol 58, 107–116. 10.1387/ijdb.130344ts. [PubMed: 25023676]
5. Spencer TE (2014). Biological roles of uterine glands in pregnancy. Semin Reprod Med 32, 346–357. 10.1055/s-0034-1376354. [PubMed: 24959816]
6. Pampfer S, and Donnay I (1999). Apoptosis at the time of embryo implantation in mouse and rat. Cell Death Differ 6, 533–545. 10.1038/sj.cdd.4400516. [PubMed: 10381643]

7. Parr EL, Tung HN, and Parr MB (1987). Apoptosis as the mode of uterine epithelial cell death during embryo implantation in mice and rats. Biol Reprod 36, 211–225. 10.1095/biolreprod36.1.211. [PubMed: 3567276]
8. Popli P, Sun AJ, and Kommagani R (2022). The Multifaceted Role of Autophagy in Endometrium Homeostasis and Disease. Reprod Sci 29, 1054–1067. 10.1007/s43032-021-00587-2. [PubMed: 33877643]
9. Yeganeh B, Lee J, Ermini L, Lok I, Ackerley C, and Post M (2019). Autophagy is required for lung development and morphogenesis. J Clin Invest 129, 2904–2919. 10.1172/JCI127307. [PubMed: 31162135]
10. Mizushima N, and Klionsky DJ (2007). Protein turnover via autophagy: implications for metabolism. Annu Rev Nutr 27, 19–40. 10.1146/annurev.nutr.27.061406.093749. [PubMed: 17311494]
11. Jang J, Wang Y, Lalli MA, Guzman E, Godshalk SE, Zhou H, and Kosik KS (2016). Primary Cilium-Autophagy-Nrf2 (PAN) Axis Activation Commits Human Embryonic Stem Cells to a Neuroectoderm Fate. Cell 165, 410–420. 10.1016/j.cell.2016.02.014. [PubMed: 27020754]
12. Xu Y, Zhang Y, Garcia-Canaveras JC, Guo L, Kan M, Yu S, Blair IA, Rabinowitz JD, and Yang X (2020). Chaperone-mediated autophagy regulates the pluripotency of embryonic stem cells. Science 369, 397–403. 10.1126/science.abb4467. [PubMed: 32703873]
13. Qu X, Zou Z, Sun Q, Luby-Phelps K, Cheng P, Hogan RN, Gilpin C, and Levine B (2007). Autophagy gene-dependent clearance of apoptotic cells during embryonic development. Cell 128, 931–946. 10.1016/j.cell.2006.12.044. [PubMed: 17350577]
14. Aburto MR, Sanchez-Calderon H, Hurle JM, Varela-Nieto I, and Magarinos M (2012). Early otic development depends on autophagy for apoptotic cell clearance and neural differentiation. Cell Death Dis 3, e394. 10.1038/cddis.2012.132. [PubMed: 23034329]
15. Cecconi F, and Levine B (2008). The role of autophagy in mammalian development: cell makeover rather than cell death. Dev Cell 15, 344–357. 10.1016/j.devcel.2008.08.012. [PubMed: 18804433]
16. Di Bartolomeo S, Latella L, Zarbalis K, and Di Sano F (2021). Editorial: Autophagy in Mammalian Development and Differentiation. Front Cell Dev Biol 9, 722821. 10.3389/fcell.2021.722821. [PubMed: 34386502]
17. Mizushima N, and Levine B (2010). Autophagy in mammalian development and differentiation. Nat Cell Biol 12, 823–830. 10.1038/ncb0910-823. [PubMed: 20811354]
18. Kuma A, Hatano M, Matsui M, Yamamoto A, Nakaya H, Yoshimori T, Ohsumi Y, Tokuhisa T, and Mizushima N (2004). The role of autophagy during the early neonatal starvation period. Nature 432, 1032–1036. 10.1038/nature03029. [PubMed: 15525940]
19. Mellen MA, de la Rosa EJ, and Boya P (2008). The autophagic machinery is necessary for removal of cell corpses from the developing retinal neuroepithelium. Cell Death Differ 15, 1279–1290. 10.1038/cdd.2008.40. [PubMed: 18369370]
20. Liang XH, Kleeman LK, Jiang HH, Gordon G, Goldman JE, Berry G, Herman B, and Levine B (1998). Protection against fatal Sindbis virus encephalitis by beclin, a novel Bcl-2-interacting protein. J Virol 72, 8586–8596. 10.1128/JVI.72.11.8586-8596.1998. [PubMed: 9765397]
21. Wang J (2008). Beclin 1 bridges autophagy, apoptosis and differentiation. Autophagy 4, 947948. 10.4161/auto.6787.
22. Wang J, Lian H, Zhao Y, Kauss MA, and Spindel S (2008). Vitamin D3 induces autophagy of human myeloid leukemia cells. J Biol Chem 283, 25596–25605. 10.1074/jbc.M801716200. [PubMed: 18628207]
23. Prerna K, and Dubey VK (2022). Beclin1-mediated interplay between autophagy and apoptosis: New understanding. Int J Biol Macromol 204, 258–273. 10.1016/j.ijbiomac.2022.02.005. [PubMed: 35143849]
24. Zhu Y, Zhao L, Liu L, Gao P, Tian W, Wang X, Jin H, Xu H, and Chen Q (2010). Beclin 1 cleavage by caspase-3 inactivates autophagy and promotes apoptosis. Protein Cell 1, 468–477. 10.1007/s13238-010-0048-4. [PubMed: 21203962]
25. Chen Y, Zhang W, Guo X, Ren J, and Gao A (2019). The crosstalk between autophagy and apoptosis was mediated by phosphorylation of Bcl-2 and beclin1 in benzene-induced hematotoxicity. Cell Death Dis 10, 772. 10.1038/s41419-019-2004-4. [PubMed: 31601785]

26. Soyal SM, Mukherjee A, Lee KY, Li J, Li H, DeMayo FJ, and Lydon JP (2005). Cre-mediated recombination in cell lineages that express the progesterone receptor. Genesis 41, 58–66. 10.1002/gene.20098. [PubMed: 15682389]
27. Gawriluk TR, Ko C, Hong X, Christenson LK, and Rucker EB 3rd (2014). Beclin-1 deficiency in the murine ovary results in the reduction of progesterone production to promote preterm labor. Proc Natl Acad Sci U S A 111, E4194–4203. 10.1073/pnas.1409323111. [PubMed: 25246579]
28. Meseguer M, Pellicer A, and Simon C (1998). MUC1 and endometrial receptivity. Mol Hum Reprod 4, 1089–1098. 10.1093/molehr/4.12.1089. [PubMed: 9872358]
29. Fullerton PT Jr., Monsivais D, Kommagani R, and Matzuk MM (2017). Follistatin is critical for mouse uterine receptivity and decidualization. Proc Natl Acad Sci U S A 114, E4772-E4781. 10.1073/pnas.1620903114.
30. Tong W, and Pollard JW (1999). Progesterone inhibits estrogen-induced cyclin D1 and cdk4 nuclear translocation, cyclin E- and cyclin A-cdk2 kinase activation, and cell proliferation in uterine epithelial cells in mice. Mol Cell Biol 19, 2251–2264. 10.1128/mcb.19.3.2251. [PubMed: 10022912]
31. Zhu L, and Pollard JW (2007). Estradiol-17beta regulates mouse uterine epithelial cell proliferation through insulin-like growth factor 1 signaling. Proc Natl Acad Sci U S A 104, 15847–15851. 10.1073/pnas.0705749104. [PubMed: 17895382]
32. Vue Z, Gonzalez G, Stewart CA, Mehra S, and Behringer RR (2018). Volumetric imaging of the developing prepubertal mouse uterine epithelium using light sheet microscopy. Mol Reprod Dev 85, 397–405. 10.1002/mrd.22973. [PubMed: 29543367]
33. Kelleher AM, DeMayo FJ, and Spencer TE (2019). Uterine Glands: Developmental Biology and Functional Roles in Pregnancy. Endocr Rev 40, 1424–1445. 10.1210/er.2018-00281. [PubMed: 31074826]
34. Kelleher AM, Peng W, Pru JK, Pru CA, DeMayo FJ, and Spencer TE (2017). Forkhead box a2 (FOXA2) is essential for uterine function and fertility. Proc Natl Acad Sci U S A 114, E1018–E1026. 10.1073/pnas.1618433114. [PubMed: 28049832]
35. Jeong JW, Kwak I, Lee KY, Kim TH, Large MJ, Stewart CL, Kaestner KH, Lydon JP, and DeMayo FJ (2010). Foxa2 is essential for mouse endometrial gland development and fertility. Biol Reprod 83, 396–403. 10.1095/biolreprod.109.083154. [PubMed: 20484741]
36. Matsuo M, Yuan J, Kim YS, Dewar A, Fujita H, Dey SK, and Sun X (2022). Targeted depletion of uterine glandular Foxa2 induces embryonic diapause in mice. Elife 11. 10.7554/eLife.78277.
37. Ni N, Gao Y, Fang X, Melgar M, Vincent DF, Lydon JP, Bartholin L, and Li Q (2018). Glandular defects in the mouse uterus with sustained activation of TGF-beta signaling is associated with altered differentiation of endometrial stromal cells and formation of stromal compartment. PLoS One 13, e0209417. 10.1371/journal.pone.0209417. [PubMed: 30550590]
38. Bellessort B, Bachelot A, Heude E, Alfama G, Fontaine A, Le Cardinal M, Treier M, and Levi G (2015). Role of Foxl2 in uterine maturation and function. Hum Mol Genet 24, 3092–3103. 10.1093/hmg/ddv061. [PubMed: 25687138]
39. Chang HJ, Shin HS, Kim TH, Yoo JY, Teasley HE, Zhao JJ, Ha UH, and Jeong JW (2018). Pik3ca is required for mouse uterine gland development and pregnancy. PLoS One 13, e0191433. 10.1371/journal.pone.0191433. [PubMed: 29346447]
40. Hayashi K, Yoshioka S, Reardon SN, Rucker EB 3rd, Spencer TE, DeMayo FJ, Lydon JP, and MacLean JA 2nd (2011). WNTs in the neonatal mouse uterus: potential regulation of endometrial gland development. Biol Reprod 84, 308–319. 10.1095/biolreprod.110.088161. [PubMed: 20962251]
41. Cooke PS, Spencer TE, Bartol FF, and Hayashi K (2013). Uterine glands: development, function and experimental model systems. Mol Hum Reprod 19, 547–558. 10.1093/molehr/gat031. [PubMed: 23619340]
42. Wong KH, Wintch HD, and Capecchi MR (2004). Hoxa11 regulates stromal cell death and proliferation during neonatal uterine development. Mol Endocrinol 18, 184–193. 10.1210/me.2003-0222. [PubMed: 14551265]

43. Cui T, He B, Kong S, Zhou C, Zhang H, Ni Z, Bao H, Qiu J, Xin Q, Reinberg D, et al. (2017). PR-Set7 deficiency limits uterine epithelial population growth hampering postnatal gland formation in mice. Cell Death Differ 24, 2013–2021. 10.1038/cdd.2017.120. [PubMed: 28731465]
44. Cousins FL, Pandoy R, Jin S, and Gargett CE (2021). The Elusive Endometrial Epithelial Stem/Progenitor Cells. Front Cell Dev Biol 9, 640319. 10.3389/fcell.2021.640319. [PubMed: 33898428]
45. Fitzgerald HC, Dhakal P, Behura SK, Schust DJ, and Spencer TE (2019). Self-renewing endometrial epithelial organoids of the human uterus. Proc Natl Acad Sci U S A 116, 23132–23142. 10.1073/pnas.1915389116. [PubMed: 31666317]
46. Turco MY, Gardner L, Hughes J, Cindrova-Davies T, Gomez MJ, Farrell L, Hollinshead M, Marsh SGE, Brosens JJ, Critchley HO, et al. (2017). Long-term, hormone-responsive organoid cultures of human endometrium in a chemically defined medium. Nat Cell Biol 19, 568–577. 10.1038/ncb3516. [PubMed: 28394884]
47. Marquez RT, and Xu L (2012). Bcl-2:Beclin 1 complex: multiple, mechanisms regulating autophagy/apoptosis toggle switch. Am J Cancer Res 2, 214–221. [PubMed: 22485198]
48. Kang R, Zeh HJ, Lotze MT, and Tang D (2011). The Beclin 1 network regulates autophagy and apoptosis. Cell Death Differ 18, 571–580. 10.1038/cdd.2010.191. [PubMed: 21311563]
49. Burton GJ, Watson AL, Hempstock J, Skepper JN, and Jauniaux E (2002). Uterine glands provide histiotrophic nutrition for the human fetus during the first trimester of pregnancy. J Clin Endocrinol Metab 87, 2954–2959. 10.1210/jcem.87.6.8563. [PubMed: 12050279]
50. Gray CA, Burghardt RC, Johnson GA, Bazer FW, and Spencer TE (2002). Evidence that absence of endometrial gland secretions in uterine gland knockout ewes compromises conceptus survival and elongation. Reproduction 124, 289–300. [PubMed: 12141942]
51. Bartol FF, Wiley AA, Floyd JG, Ott TL, Bazer FW, Gray CA, and Spencer TE (1999). Uterine differentiation as a foundation for subsequent fertility. J Reprod Fertil Suppl 54, 287–302. [PubMed: 10692862]
52. Levine B, and Klionsky DJ (2004). Development by self-digestion: molecular mechanisms and biological functions of autophagy. Dev Cell 6, 463–477. 10.1016/s1534-5807(04)00099-1. [PubMed: 15068787]
53. Mizushima N, and Komatsu M (2011). Autophagy: renovation of cells and tissues. Cell 147, 728–741. 10.1016/j.cell.2011.10.026. [PubMed: 22078875]
54. Lee E, Koo Y, Ng A, Wei Y, Luby-Phelps K, Juraszek A, Xavier RJ, Cleaver O, Levine B, and Amatruda JF (2014). Autophagy is essential for cardiac morphogenesis during vertebrate development. Autophagy 10, 572–587. 10.4161/auto.27649. [PubMed: 24441423]
55. Jung HS, Chung KW, Won Kim J, Kim J, Komatsu M, Tanaka K, Nguyen YH, Kang TM, Yoon KH, Kim JW, et al. (2008). Loss of autophagy diminishes pancreatic beta cell mass and function with resultant hyperglycemia. Cell Metab 8, 318–324. 10.1016/j.cmet.2008.08.013. [PubMed: 18840362]
56. Hou W, Han J, Lu C, Goldstein LA, and Rabinowich H (2010). Autophagic degradation of active caspase-8: a crosstalk mechanism between autophagy and apoptosis. Autophagy 6, 891–900. 10.4161/auto.6.7.13038. [PubMed: 20724831]
57. Liu Y, and Levine B (2015). Autosis and autophagic cell death: the dark side of autophagy. Cell Death Differ 22, 367–376. 10.1038/cdd.2014.143. [PubMed: 25257169]
58. Dunlap KA, Filant J, Hayashi K, Rucker EB 3rd, Song G, Deng JM, Behringer RR, DeMayo FJ, Lydon J, Jeong JW, and Spencer TE (2011). Postnatal deletion of Wnt7a inhibits uterine gland morphogenesis and compromises adult fertility in mice. Biol Reprod 85, 386–396. 10.1095/biolreprod.111.091769. [PubMed: 21508348]
59. Mericskay M, Kitajewski J, and Sassoon D (2004). Wnt5a is required for proper epithelial-mesenchymal interactions in the uterus. Development 131, 2061–2072. 10.1242/dev.01090. [PubMed: 15073149]
60. Stewart CA, Wang Y, Bonilla-Claudio M, Martin JF, Gonzalez G, Taketo MM, and Behringer RR (2013). CTNNB1 in mesenchyme regulates epithelial cell differentiation during Mullerian duct and postnatal uterine development. Mol Endocrinol 27, 1442–1454. 10.1210/me.2012-1126. [PubMed: 23904126]

61. Kurita T, Cooke PS, and Cunha GR (2001). Epithelial-stromal tissue interaction in paramesonephric (Mullerian) epithelial differentiation. Dev Biol 240, 194–211. 10.1006/dbio.2001.0458. [PubMed: 11784056]
62. Cunha GR, Battle E, Young P, Brody J, Donjacour A, Hayashi N, and Kinbara H (1992). Role of epithelial-mesenchymal interactions in the differentiation and spatial organization of visceral smooth muscle. Epithelial Cell Biol 1, 76–83. [PubMed: 1307941]
63. Cunha GR, Young P, and Brody JR (1989). Role of uterine epithelium in the development of myometrial smooth muscle cells. Biol Reprod 40, 861–871. 10.1095/biolreprod40.4.861. [PubMed: 2752077]
64. Seishima R, Leung C, Yada S, Murad KBA, Tan LT, Hajamohideen A, Tan SH, Itoh H, Murakami K, Ishida Y, et al. (2019). Neonatal Wnt-dependent Lgr5 positive stem cells are essential for uterine gland development. Nat Commun 10, 5378. 10.1038/s41467-019-13363-3. [PubMed: 31772170]
65. Cousins FL, O DF, and Gargett CE (2018). Endometrial stem/progenitor cells and their role in the pathogenesis of endometriosis. Best Pract Res Clin Obstet Gynaecol 50, 27–38. 10.1016/j.bpobgyn.2018.01.011. [PubMed: 29503126]
66. Wu B, An C, Li Y, Yin Z, Gong L, Li Z, Liu Y, Heng BC, Zhang D, Ouyang H, and Zou X (2017). Reconstructing Lineage Hierarchies of Mouse Uterus Epithelial Development Using Single-Cell Analysis. Stem Cell Reports 9, 381–396. 10.1016/j.stemcr.2017.05.022. [PubMed: 28625536]
67. Boya P, and Kroemer G (2009). Beclin 1: a BH3-only protein that fails to induce apoptosis. Oncogene 28, 2125–2127. 10.1038/onc.2009.83. [PubMed: 19398951]
68. Ciechomska IA, Goemans GC, Skepper JN, and Tolkovsky AM (2009). Bcl-2 complexed with Beclin-1 maintains full anti-apoptotic function. Oncogene 28, 2128–2141. 10.1038/onc.2009.60. [PubMed: 19347031]
69. Rocchi A, Yamamoto S, Ting T, Fan Y, Sadleir K, Wang Y, Zhang W, Huang S, Levine B, Vassar R, and He C (2017). A Becn1 mutation mediates hyperactive autophagic sequestration of amyloid oligomers and improved cognition in Alzheimer's disease. PLoS Genet 13, e1006962. 10.1371/journal.pgen.1006962. [PubMed: 28806762]
70. Wang C, Haas M, Yeo SK, Sebti S, Fernandez AF, Zou Z, Levine B, and Guan JL (2022). Enhanced autophagy in Becn1(F121A/F121A) knockin mice counteracts aging-related neural stem cell exhaustion and dysfunction. Autophagy 18, 409–422. 10.1080/15548627.2021.1936358. [PubMed: 34101533]
71. Kommagani R, Szwarc MM, Kovanci E, Gibbons WE, Putluri N, Maity S, Creighton CJ, Sreekumar A, DeMayo FJ, Lydon JP, and O'Malley BW (2013). Acceleration of the glycolytic flux by steroid receptor coactivator-2 is essential for endometrial decidualization. PLoS Genet 9, e1003900. 10.1371/journal.pgen.1003900. [PubMed: 24204309]
72. Chadchan SB, Cheng M, Parnell LA, Yin Y, Schriefer A, Mysorekar IU, and Kommagani R (2019). Antibiotic therapy with metronidazole reduces endometriosis disease progression in mice: a potential role for gut microbiota. Hum Reprod 34, 1106–1116. 10.1093/humrep/dez041. [PubMed: 31037294]
73. Xu R, Boreland AJ, Li X, Erickson C, Jin M, Atkins C, Pang ZP, Daniels BP, and Jiang P (2021). Developing human pluripotent stem cell-based cerebral organoids with a controllable microglia ratio for modeling brain development and pathology. Stem Cell Reports 16, 1923–1937. 10.1016/j.stemcr.2021.06.011. [PubMed: 34297942]
74. Kommagani R, Szwarc MM, Vasquez YM, Peavey MC, Mazur EC, Gibbons WE, Lanz RB, DeMayo FJ, and Lydon JP (2016). The Promyelocytic Leukemia Zinc Finger Transcription Factor Is Critical for Human Endometrial Stromal Cell Decidualization. PLoS Genet 12, e1005937. 10.1371/journal.pgen.1005937. [PubMed: 27035670]
75. Liu J, Xia H, Kim M, Xu L, Li Y, Zhang L, Cai Y, Norberg HV, Zhang T, Furuya T, et al. (2011). Beclin1 controls the levels of p53 by regulating the deubiquitination activity of USP10 and USP13. Cell 147, 223–234. 10.1016/j.cell.2011.08.037. [PubMed: 21962518]
76. Deane JA, Ong YR, Cain JE, Jayasekara WS, Tiwari A, Carlone DL, Watkins DN, Breault DT, and Gargett CE (2016). The mouse endometrium contains epithelial, endothelial and leucocyte populations expressing the stem cell marker telomerase reverse transcriptase. Mol Hum Reprod 22, 272–284. 10.1093/molehr/gav076. [PubMed: 26740067]

Highlights

- Endometrial Beclin-1 is essential for uterine development and pregnancy establishment.
- Endometrial progenitor stem cell maintenance requires Beclin-1.
- Intrinsic autophagy is indispensable for uterine adenogenesis.
- Beclin-1-mediated autophagy but not apoptosis governs postnatal uterine morphogenesis.

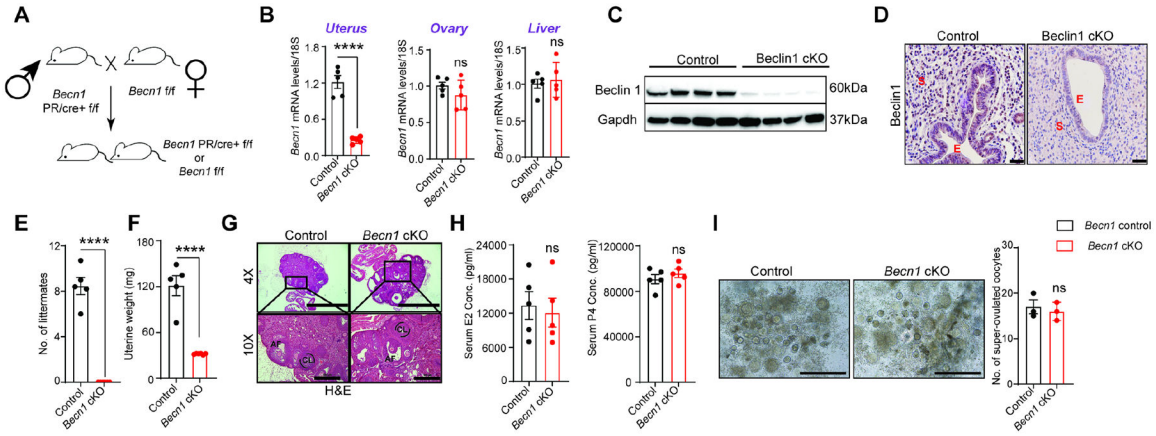

Figure 1: Conditional ablation of *Becn1* results in female infertility with intact ovarian function.

(**A**) Mouse breeding strategy employed to generate control (*Becn1*$^{f/f}$) mice or *Becn1*$^{f/f}$;PR$^{cre/+}$ (*Becn1* cKO) mice. (**B**) Relative transcript levels of *Becn1* in 8-week-old virgin control and cKO uteri (whole uterus including epithelial, stromal, and myometrial compartment), ovary, and liver (n=6). mRNA levels are normalized to levels of 18S m-RNA. Data are presented as mean ± SEM; ***P<0.001, P>0.05, ns=non-significant. (**C & D**) *Left panel*, Western blotting to show protein levels of Beclin-1 in uteri from 8-week-old virgin control and cKO uteri. GAPDH is used as a loading control. *Right panel*, Immunohistological analysis of Beclin-1 expression in Control and *Becn1* cKO mice. Scale bar: 40 μm (**E & F**) Relative number of littermates and uterine weight of *Becn1* control and cKO mice sacrificed after breeding trial. Data are presented as mean ± SEM; P>0.05, ns=non-significant. (**G**) H&E staining of ovaries from 8-week-old control and *Becn1* cKO mice; scale bar: 2mm (upper panel), 500 μm (lower panel) (**H**) Levels of reproductive hormones estradiol and progesterone from serum collected during euthanasia of 8-week-old virgin mice. (**I**) Super-ovulated oocytes retrieved from 4-week-old *Becn1* control and cKO mice (*left*). Number of super-ovulated oocytes in 4-week-old control and *Becn1* cKO mice (*Right*); scale bar: 200 μm

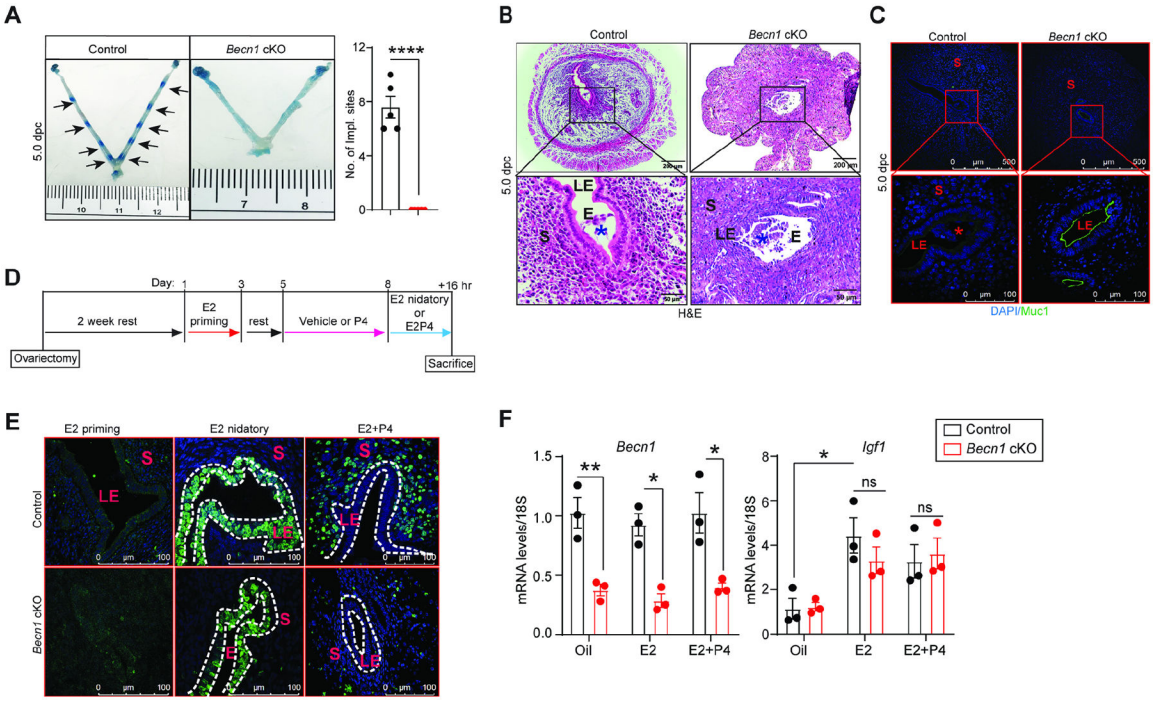

Figure 2: *Becn1* is critical for embryo implantation and uterine receptivity.

(**A**) Images of 5.0 dpc uteri of control and *Becn1* cKO mice injected with Chicago Sky Blue dye to visualize implantation sites (denoted by black arrows) (*Left*). Quantification of implantation sites in control (n=6) and *Becn1* cKO (n=6) mice on day 5 of pregnancy (*Right*). (**B**) H&E-stained cross-sections of 5.0 dpc uteri of control and *Becn1* cKO mice to visualize embryo implantation. LE, luminal epithelium; S, stroma. Asterisk denotes the embryo. Scale bar: 200 μm, 50 μm (**C**) Immunofluorescence analysis of uterine tissues from Control and *Becn1* cKO mice, stained with Muc1. scale bar: 500 μm, 100 μm. (**D**) Experimental protocol for hormonal induction of uterine receptivity in ovariectomized mice. (**E**) Representative immunofluorescence images of uteri from Control and *Becn1* cKO mice stained for Ki-67 following Oil or E2 or E2+P4 treatment (n = 5 mice/group); scale bar: 100 μm. (**F**) Transcript levels of *Becn1* and *Igf1*, in uteri from Control and *Becn1 c*KO mice in the indicated treatment groups. Data are presented as mean ± SEM (n = 5), P>0.05, ns=non-significant.

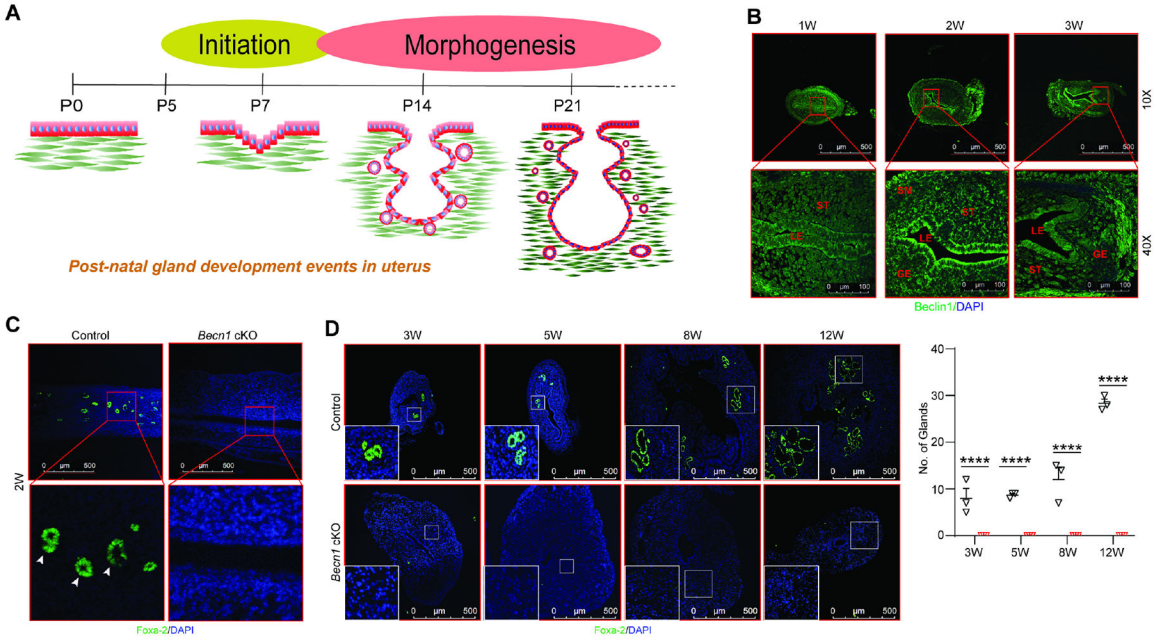

Figure 3: *Becn1* is indispensable for uterine glandular development and morphogenesis.

(A) Graphical illustration to show gland development events in uterus **(B)** Immunofluorescence analysis to show Beclin-1 expression in 1 to 3-week (W)-old control and *Becn1* cKO uteri; scale bar: 500 μm, 100 μm (C & D) Immunofluorescence analysis to show Foxa2-positive glandular structures in uteri from Control and *Becn1* cKO at 2W of age (lower panel showing magnified images) and different PNDs (3 to 12W) of development (*left*); scale bar: 500 μm. Quantitative analysis of Foxa2-positive glands on indicated PNDs. Data represents the number of glands counted from four different areas of uterine cross-sections; images taken at 100X magnification and the average number of glands from n=3 mice was presented. Data shown represent the mean± S.E.M., *P>0.05, ns=non-significant.

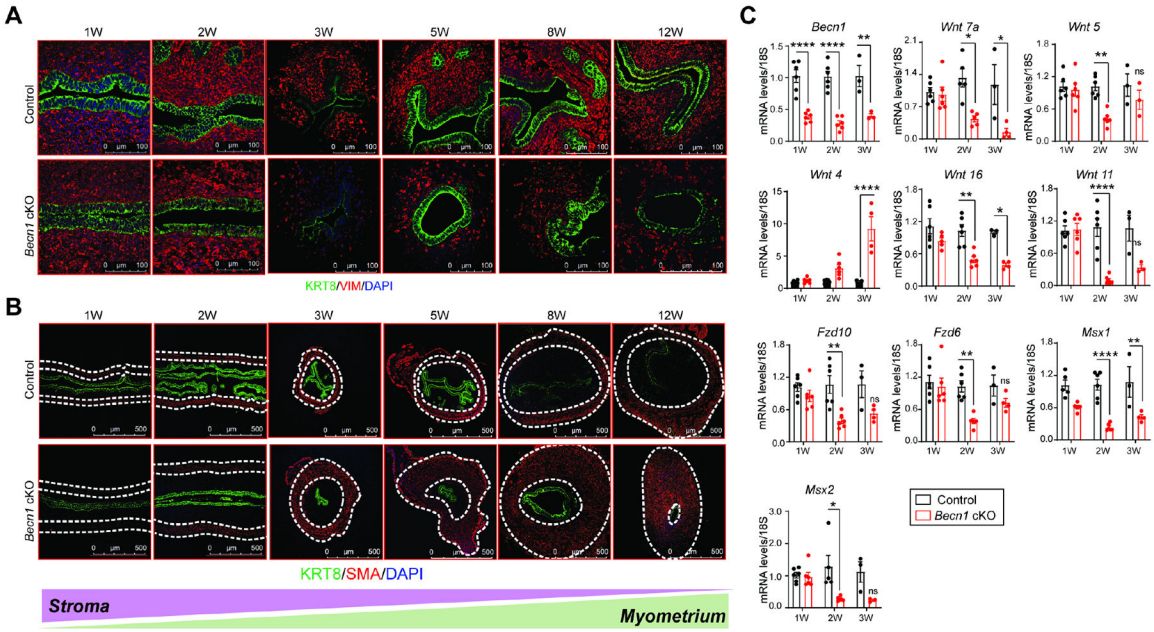

Figure 4: Loss of *Becn1* leads to undifferentiated stroma and myometrium resulting in hyper-muscular uteri.

(**A**) Immunolocalization of KRT8 (green) and Vimentin (red) in the uteri of Control and *Becn1* cKO at different PNDs; scale bar: 100 μm (**B**) Immunofluorescence of KRT8 (green) and smooth muscle α-actin (red) in the uteri of Control and *Becn1* cKO at different PNDs. DAPI (blue) was used to counterstain the nuclei; scale bar: 500 μm (**C**) Relative mRNA expression of genes implicated in uterine development at different PNDs from Control and *Becn1* cKO mice.

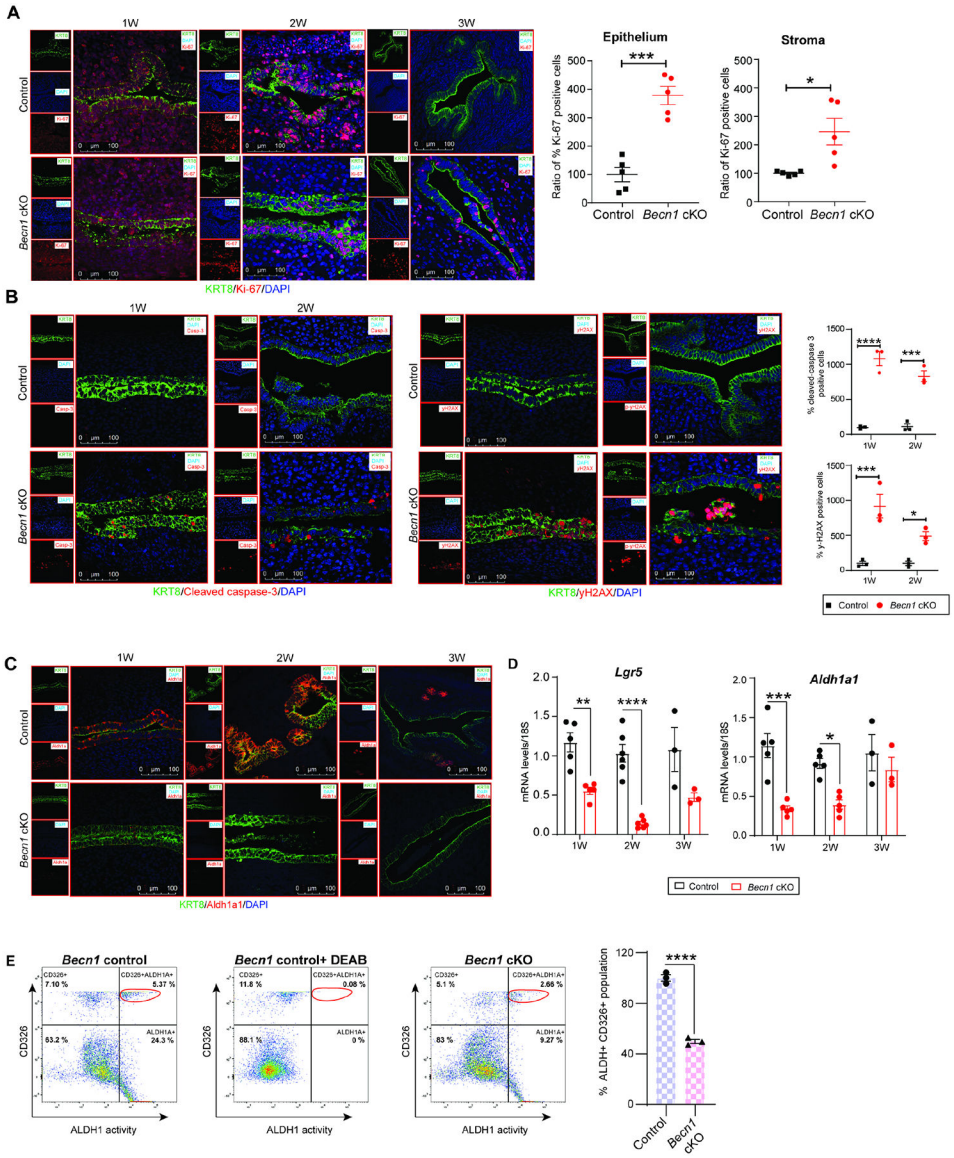

Figure 5: Endometrial progenitor stem cell maintenance requires *Becn1* during early uterine morphogenesis.

(**A**) Immunofluorescence of KRT8 (green) and Ki67 (red) in uteri of Control and *Becn1* cKO mice at 1, 2 and 3W of postnatal stage of uterus development (*left*); scale bar: 100 μm. Quantification of Ki67-positively stained cells in the luminal epithelia and stromal compartment of uteri at 3W of postnatal age. Data represents the ratio of the number of Ki67-positive cells to the total number of cells counted in four different areas and plotted as percent positive cells from n=6 mice (*right*). (**B**) Immunofluorescence of KRT8 (green), cleaved caspase-3 (red), and γH2AX in uteri of Control and *Becn1* cKO mice during 1W, and 2W of postnatal age of uterus development (*left*); scale bar: 100 μm. Quantification of cleaved caspase-3 and γH2AX-positively stained epithelial cells in uteri at 1W, and 2W of postnatal ages. Data represents the ratio of the number of positive cells to the total number of cells counted in four different areas and plotted as percent positive cells from n=3 mice (*right*). (**C**) Immunolocalization of endometrial progenitor stem cell marker;

Aldh1a1 in uteri at different PNDs (*upper panel*); scale bar: 100 μm (**D**) Transcript levels of endometrial progenitor stem cell markers *Aldh1a1* and *Lgr5* during the critical window of uterine maturation. (**E**) Representative flow cytometry analysis of ALDH1A1 activity in uterine cells isolated from *Becn1* 2W old control and cKO uteri. Control cells treated with DEAB was used as negative control for Aldefluor staining.

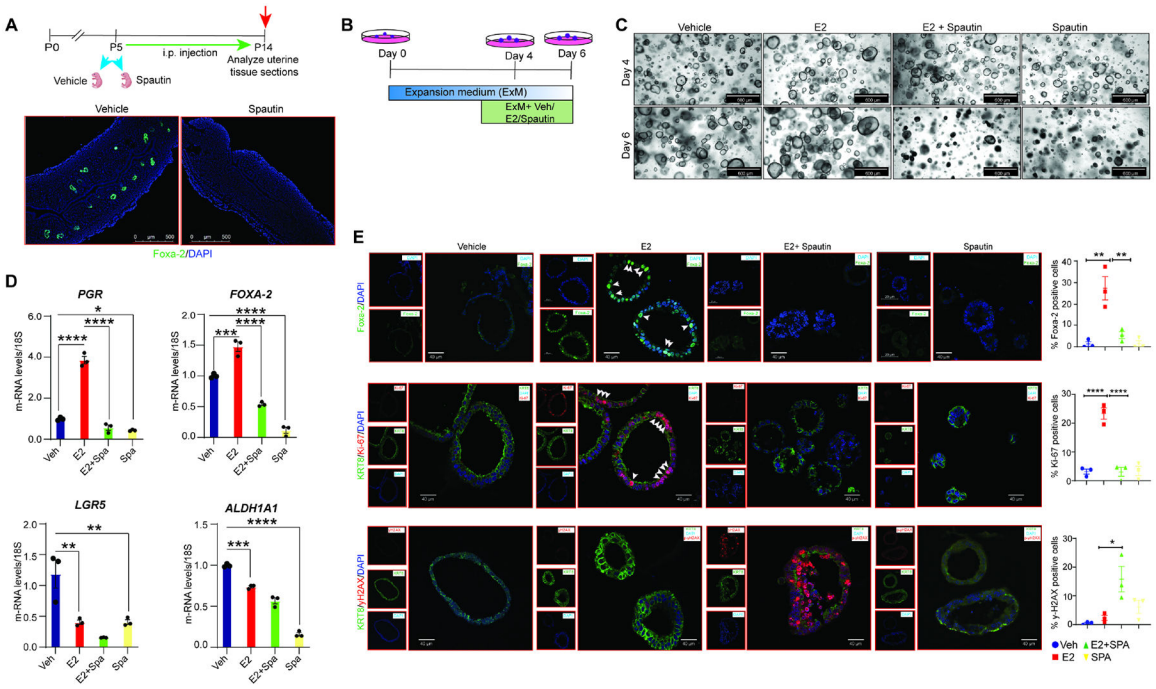

Figure 6: Pharmacological inhibition of autophagy impedes uterine glandular development in mice and human organoids.

(**A**) (*Upper panel*) Experiment strategy to inhibit autophagy in neonatal uteri. Mice pups were treated with Vehicle or Spautin on PND5 and euthanized at PND14 time-point for tissue harvesting (*Lower panel*). Immunofluorescence imaging to show Foxa2 (green)-positive glandular structures in Vehicle or Spautin-treated 2W old WT mice pups. DAPI (blue) was used to counterstain the nuclei; scale bar: 500 μm. (**B**) Experimental timeline of human endometrial epithelia organoid cultures. Organoids were derived in ExM and then subjected to treatment with Vehicle or E2 or E2+Spautin or Spautin alone. (**C**) Representative bright-field images showing morphology of endometrial organoids prior to treatment on day 4 or after treatment with Vehicle or E2 (10nM) or E2 (10nM) +Spautin (15 μM) or Spautin (15 μM) alone for two days on day 6; scale bar: 600 μm (**D**) Relative mRNA levels of *PGR*, *FOXA2, LGR5* and ALDH1A1 in hormone-or Spautin-treated organoids. Data are means ± SEMs. *P ≤ 0.05, **P ≤ 0.01, ***P ≤ 0.001, ****P ≤ 0.0001. (**E**) *(left)* Immunolocalization of FOXA2, KRT8 (Green)+ Ki-67 (Red), KRT8 (Green)+ γH2AX (Red) in response to E2 or Spautin inhibitor. Organoids were counterstained with DAPI (blue) to visualize nuclei, scale bar: 40 μm. Quantification of the percentage of FOXA2, Ki-67 and γH2AX positive cells relative to the total number of cells in organoid sections *(right)*. Three independent experiments were performed and for each experiment, 7–10 organoids per treatment group were counted and plotted as percent positive cells. Data are presented as mean ± SE.

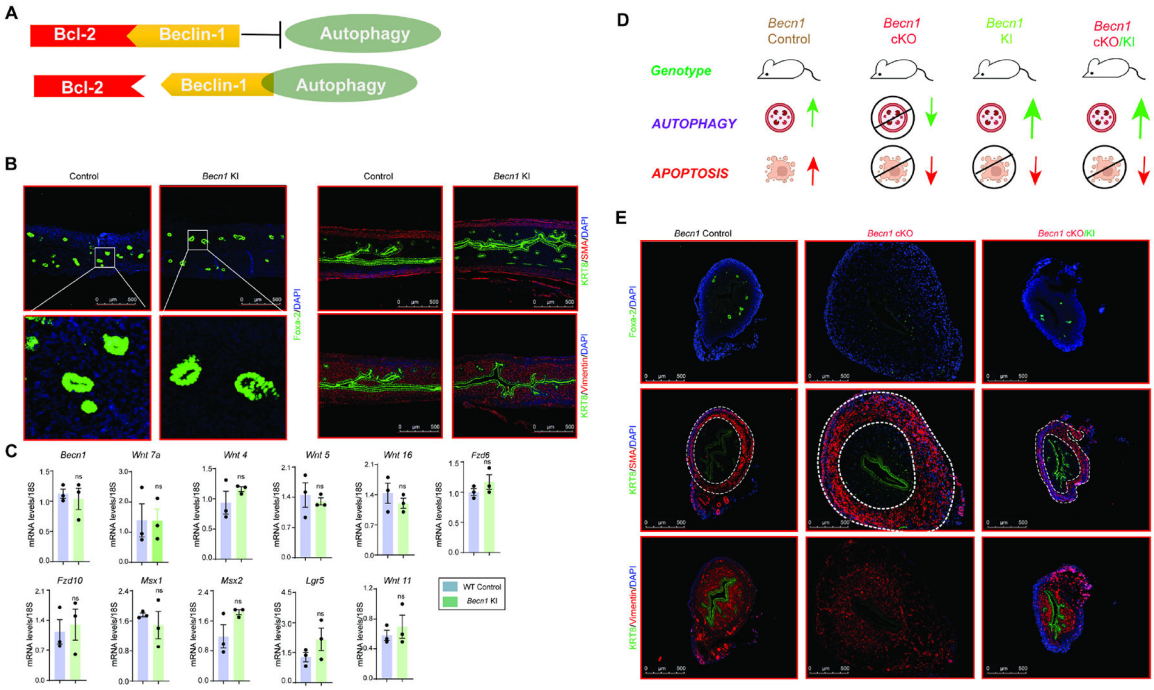

Figure 7: *Becn1*-dependent autophagy but not apoptosis is required for postnatal uterine gland development in mice.

(**A**) Illustration of Beclin-1-Bcl2 interaction (**B**) Immunolocalization of Foxa2-positive glandular structures in upper panel and magnified images in lower panel; scale bar: 500 μm. Immunofluorescence of KRT8 (Green)+ Vimentin (Red), KRT8 (Green)+ smooth muscle α-actin (Red) in uteri from control wild-type and *Becn1* KI mice by 2W of postnatal age of development. DAPI (blue) was used to counterstain the nuclei; scale bar: 500 μm (**C**) Transcript levels of various candidate genes associated with gland development and uterine maturation. (**D**) Graphical illustration to demonstrate Beclin-1-dependent autophagy or apoptosis in different genetically engineered mice. (**E**) Immunolocalization of Foxa2 (Green), KRT8 (Green)+ SM-α-actin (Red), KRT8 (Green)+ Vimentin (Red) in *Becn1* control, cKO and cKO/KI mice; scale bar: 500 μm.

Table 1:

Six-month breeding trial with wild-type males

Genotype	Females	Pups	Pups/female	Litters	Pups/litter
Control	n=5	181	36±0.68	21	8.6±2.52
Becn1 cKO	n=6	0	0	0	0

Key resources table

REAGENT or RESOURCE	SOURCE	IDENTIFIER
Antibodies		
Beclin	Cell Signaling Technology	#3495T
Beclin	Novus Biologicals	NB500–249
ER-α	Abcam	ab75635
PR	Santa cruz Biotechnology	sc-538 PR (C-19
Normal Rabbit IgG	Cell Signaling Technology	#2729
GAPDH	Cell Signaling Technology	#2118S
Anti-rabbit IgG, HRP-linked	Cell Signaling Technology	#7074
KRT8	Developmental Studies Hybridoma Bank	TROMA-I
Smooth muscle α-actin	Abcam	ab5694
Vimentin	Abcam	ab92547
ALDH1A	Abcam	ab52492
Muc1	Abcam	ab15481
Foxa-2	Abcam	ab108422
Ki-67	Abcam	ab16667
Cleaved caspase 3	Cell Signaling Technology	9664s
p-YH2AX	Cell Signaling Technology	9718s
Biological samples		
Human endometrial tissue	Baylor College of Medicine	IRB ID #: H-21138
Chemicals, peptides, and recombinant proteins		
Spautin-1	Selleck chemicals	Catalog No: S7888
Critical commercial assays		
ALDEFLUOR™ Kit	Stem Cell technologies	Catalog # 01700
Experimental models: Organisms/strains		
$Beclin^{flox/flox}$ mice	Dr. Edmund B. Rucker, University of Kentucky, Lexington, KY 40506, USA (Gawriluk et al., 2014)[27]	N/A
Becn1$^{F121A/F121A}$ (*Becn1* KI)	Dr. Christina Stallings, Washington University School of Medicine, St. Louis, MO, 63110, USA (Rocchi et al., 2017)[69]	N/A
$Beclin^{flox/flox}$; $PR^{cre/+}$ mice (*Becn1* cKO)	This manuscript	N/A
$Beclin^{flox/+}$; $PR^{cre/+}$/*Becn1*$^{F121A/+}$ mice (*Becn1* cKO/KI)	This manuscript	N/A
Oligonucleotides – Refer to Supplementary Table S1		
Software and algorithms		
GraphPad Prism version 9.5.0	N/A	https://www.graphpad.com/
Fiji (ImageJ)	N/A	https://imagej.nih.gov/ij/
Other		
Pierce BCA Protein Assay Kit	Thermo Fisher Scientific	Cat#23225
16% Formaldehyde solution	Thermo Fisher Scientific	28908

REAGENT or RESOURCE	SOURCE	IDENTIFIER
4–15% Mini-PROTEAN® TGX™ Precast Protein Gels	BioRad	#4561083
Pierce™ ECL Western Blotting Substrate	Thermo Fisher Scientific	32209